Compression Testing of Ceramic Foam Filters (CFFs) Submerged in Aluminium at Operating Temperature

Are Bergin[1 2], Robert Fritzsch[1], Shahid Akhtar[3], Lars Arnberg[1] and Ragnhild E. Aune[1]

[1]Dept. of Materials Science and Engineering, Norwegian University of Science and Technology (NTNU), Trondheim, NORWAY

[2]Hydro Aluminium AS, Research and Technology Development, Sunndalsøra, NORWAY

[3]Hydro Aluminium AS, Karmøy Primary Production, Håvik, NORWAY

Communicating author: Are Bergin (are.bergin@ntnu.no, are.bergin@hydro.com)

Abstract

Particles and inclusions are commonly removed from molten aluminium with the use of Ceramic Foam Filters (CFF). The mechanical properties of CFFs are of great importance not only during transportation, storage and mounting, but also in view of securing the integrity of the filters during operation. Data on the compression strength of CFFs at room temperature are available in literature, but this is not the case for their performance under operating conditions. The main aim of the present study has therefore been to develop an experimental procedure enabling compression testing of CFFs submerged in molten aluminium at operating temperature, *i.e.* when exposed to actual casthouse conditions. The effect of temperature and holding time was investigated with tests performed at room temperature, at operating temperature with varying duration of filter sample preheating, and submerged in molten aluminium. The developed procedure for the measurement of the compression strength for samples submerged in aluminium showed realistic and reproducible data in comparison with previous studies and testing at room temperature. The filter tested was a commercial 30 ppi Al_2O_3-based CFF, which as expected revealed a significant decrease in compression strength for the filter samples submerged in aluminium. The weakened structure of the ceramic foam is believed to be due to a reaction occurring between the CFF and the molten aluminium. Additionally, the exposed filter samples also exhibited a less brittle behaviour compared to the unexposed samples, indicating that even a softening of the ceramic structure had taken place.

Key words: Filtration, Ceramic Foam Filters (CFFs), Mechanical strength, Compression Strength, Cracking.

1. Introduction

Ceramic foams exist in numerous shapes and compositions depending on the application, and one example is as filtration media during molten metal filtration. Ceramic Foam Filters (CFFs) are usually produced using the replica method patented by Schwartzwalder *et al.* [1], where a polyurethane foam is coated with a ceramic slurry with subsequent sintering. In the sintering step the polyurethane foam is decomposed leaving a ceramic foam replicating the polymer foam. The remaining ceramic structure is a network of struts and pores/cells, where the former are circular beams that are hollow and holds the network together while the pores/cells are holes or half-spheres allowing the molten metal to flow through. An important filtration parameter is the functional pore size of the CFFs specified by the producer in ppi (pores per inch) or grades. The higher the ppi number, the smaller are the functional pores which results in a higher filtration efficiency [2]. During handling and filtration, the CFFs have to withstand mechanical and thermo-mechanical stresses. In order to

make predictions about the suitability of a special filter and as quality control, the compression strength of the CFFs can be tested.

During compression testing of foams, Ashby describes the resulting stress-strain curves having three regions, *i.e.* linear elasticity, collapse and densification [3]. The linear elasticity occurs at low strains and is described by bending of cell walls and struts, which is followed by the collapse described to occur at almost constant stress (a plateau) and is where the cell walls and struts fracture. These two regions were also described experimentally by Meille *et al.* [4] during compression testing of porous alumina samples, while Dam *et al.* [5] reported that the 2nd region was substantially different and varied significantly between samples during compression of alumina-mullite ceramic foams. Voigt *et al.* [6] defined overall failure and structural collapse of alumina ceramic foams by a force loss of 70 % of the maximum force, and this was confirmed by observations of the foam actually breaking into pieces. This description of overall failure is supported by other authors [5,7], which describe a load drop due to propagation of macroscopic cracks at the crushing point of cordierite and alumina-mullite ceramic foams. Furthermore, the region of linear elasticity can be reviewed considering previous experimental work, where it has been reported that prior to overall failure there are local failures of single struts occurring [6–9].

According to Ashby [3], the most important aspect considering the structure of foams is the relative density (ρ_{rel}), which is the parameter that the mechanical properties of foams above all else depend on (regardless of if the structure consists of open or closed cells). The relative density is defined as:

$$\rho_{rel} = \frac{\rho_{foam}}{\rho_{solid}} \tag{1}$$

where ρ_{foam} is the density of the entire foam and ρ_{solid} the density of the solid that the foam is constructed from, the latter also being referred to as the material density.

The correlation between the compression strength (σ_{fc}) of a brittle foam and the relative density was proposed by Gibson and Ashby [3,10] to be as follows:

$$\sigma_{fc} = C \cdot \sigma_{mf} \cdot \left(\frac{\rho_{foam}}{\rho_{solid}}\right)^{3/2} \tag{2}$$

where σ_{mf} is the fracture strength of the material by which the foam is constructed and C a constant. The theory of an increasing compression strength with increasing relative density has been proven by numerous researchers [4,5,8,11,12]. The exponent of the relative density in Equation (2) however, has been described by Oliveira *et al.* [7] to vary from 2.2 to 3.6 for different experimental studies.

Interestingly, Ashby states that the effect of defects such as flaws, cracks and variations in pore size on the compressive fracture of foams, is low [3]. This has however, been questioned by several researchers [5,7,12–14] stating that flaws have a clear detrimental effect on both the strength and the variability of the results. The order of magnitude for the detrimental effect flaws has on the strength of ceramic foams have been described by other authors [7,13], which also states that larger samples would fail at lower stresses compared to smaller samples as the probability of the larger samples containing pre-existing flaws would be higher. Additionally, Voigt *et al.* [6] tested CFFs with different homogeneity with regard to the porosity, where the homogenous foams had a difference in porosity between the middle and the outer parts of the foam of 2 % and the inhomogeneous of 19 %, and showed that the compression strength of the homogeneous filters were three to four time higher than that of the inhomogeneous filters.

Flaws and cracks will necessarily occur in struts due to the shrinkage during sintering. Additionally, in mechanical models the struts are often assumed to possess the same properties as the bulk solid without being hollow. Dam *et al.* [5] confirmed through observations that foam fracture occurred either as a transverse failure of struts or longitudinal strut splitting, suggesting that a more detailed view of the struts (than described in Equation (2)) is important. Brezny *et al.* [14] proposed a relationship for the calculation of strut strength (σ_{sf}) through measurements of the struts outer and inner (hollow strut centre) dimensions, as well as the load at strut fracture for high purity alumina and alumina-10 % zirconia ceramic foams:

$$\sigma_{sf} = \frac{36 \cdot P \cdot L \cdot D}{9 \cdot \pi \cdot D^4 - 16 \cdot b \cdot h^3} \quad (3)$$

where P is the fracture load, L the strut length, D the strut outside diameter, while b and h are the base and height of the hollow strut centre which is triangular. The results presented by Brezny *et al.* [14] showed that the strut dimensions remained constant regardless of an increase in foam density, as higher additions of solids lead to formation of cell faces and closed pores, and thus a constant strut strength was obtained even with changes in the density of the ceramic foam. The concept of constant strut diameter with increasing relative densities was further supported by Brezny *et al.* [13] for alumina- and alumina-10 % zirconia foams, and later by Dam *et al.* [5] for an alumina-mullite ceramic foam. The observed independence of strut size on density is, however, not to be mistaken for an independence of strut size on pore size, as a decrease in the ppi does increase the length and thickness of the struts as measured by Brezny *et al.*[15].

Based on the finite element method Voigt *et al.* [6] performed calculations of the stress distribution of ceramic foams between loading plates, and reported stress peaks in close proximity to the loading plates, suggesting that failure would occur there. It was further assumed that for an increase in pore size, the mentioned stress peaks would be reduced, leading to a homogenous stress distribution where failure was just as likely through the whole thickness of the foam rather than only at the layers closest to the loading plates. In a later in-situ experimental study by Hubálková *et al.*[9], X-ray microtomography was used to carefully study compression testing of alumina ceramic foams, and it was observed that the failure occurred close to the loading plates. This was explained as an obvious phenomenon as the struts in contact with the loading plates would be exposed to a force five times higher than the applied compression stress when the porosity of the tested foams was 80 %.

Voigt *et al.* [6] conducted an extensive study on how different parameters influenced the compressive strength during testing of porous alumina ceramic foams. Amongst other things, they reported that an increase in the foam compression strength was obtained as a result of an increase in sample size and a decrease in the size of the loading plates. The latter can be explained by a failure mechanism described by Gibson *et al.* [10], where they propose that there is a linear dependence between the compression strength and the square root of the loaded area. The experimental observations by Voigt *et al.* [6] were further supported by simulations using the finite element method (Abaqus). An increasing compression strength with increasing sample size, was also reported by Heness *et al.* [16] in an experimental study on porous ceramic insulating bricks consisting mainly of alumina and silica. This contradicts the previously described assumption that larger samples would have lower strength due to higher probability of flaws in the structure. This implies that compression strength values for ceramic foams cannot be directly compared, except if the sample shape and size, as well as the loaded area, is identical. Additionally, it was reported by Voigt *et al.* [6] that there were very little or no effect on the rate of applied load on the compression strength of ceramic foams.

It should be noted that in regard to the effect of the pore size on the compression strength of ceramic foams, *i.e.* of the ppi/grade in the case of CFFs, there is no clear trend described in literature. According to Oliveira *et al.* [7] an increase in the mechanical strength of the ceramic foam will be the result of reduced porosity which can be explained by an overall reduction of the pore size. Experimental observations made by other researchers have, however, shown an inconsistent connection where an increase in pore size has been described to decrease the compression strength by some researchers [4,15] and increase the compression strength by others [5], while Voigt *et al.* [6] observed small differences without a specific trend.

There is limited literature on compression strength of ceramic foams at elevated temperature. Goretta *et al.* [11], however, performed an experimental study on alumina ceramic foams in air at room temperature and at temperatures between 800℃ and 1500 ℃ by equilibrating the samples at test temperatures for 30 minutes. The compression strength was reported to be similar to room temperature at 800 ℃, increase at 900 ℃, and then again to be similar to room temperature in the interval 1000 – 1200 ℃, and then finally decreasing again at temperatures >1200 ℃. The results were explained by the fact that alumina consists of a glassy phase that increases in strength at 900 ℃ as a result of glass softening that covers the flaws in the ceramic structure, while the decrease in strength >1200 ℃ is an effect of further glass softening that would decrease the viscosity of the glassy phase.

Similar to the limited amount of literature available at elevated temperatures for CFFs, there are no studies investigating the compression strength at operating conditions, *i.e.* in contact with molten metal. As it potentially could be large

differences in the filter strength in air at elevated temperatures compared to in contact with molten metal at operating temperatures, the present study aims at developing an experimental procedure enabling compression testing of CFFs at operating temperature and submerged in molten aluminium securing reproducible results. The outcome of the study is believed to be of significant importance for both CFF suppliers, as well as aluminium producers.

2. Experimental Procedures and Materials

2.1 Characterisation of the Ceramic Foam Filter (CFF)

All tested samples were retrieved from the same filter type, which was an Al_2O_3-based CFF with a pore size of 30 ppi supplied by Pyrotek Sivex (Czech Republic). The filter was characterised as-received by an Ultra 55 LE (Zeiss, Germany) scanning electron microscope (SEM), and analysis of the chemical composition was secured by using an XFlash Detector 4010 (Bruker AXS, Germany) energy-dispersive X-ray microanalysis unit (EDS). In addition, measurements of the filter porosity were obtained using an Autopore 5 (Micromeritics, USA) mercury intrusion porosimetry unit (MIP), and of the strut thickness using a VHX-2000 digital microscope (Keyence, Japan).

The chemical composition presented for the samples is the average of 7 measurements at a size of ~ 200 x 200 μm^2 using an accelerating voltage of 20 kV and a 10 mm working distance. The mercury intrusion porosimetry was performed using a penetrometer with a cup volume of 15 cm^3 and a stem volume of 0.392 cm^3 which enabled analysis of relatively large samples (> 10 x 10 x 10 mm^3). A total of 295 measuring points ranging between 0.15 MPa and 420 MPa, and an equilibrium time of 5 seconds were used. The measured pressure (p) was converted into the corresponding pore radius (r) with the help of Washburn's equation:

$$p = (2 \cdot \gamma \cdot \cos \theta) / r \tag{4}$$

where θ is the contact angle and γ the surface tension of mercury. In the present case $\theta = 140°$ and $\gamma = 0.485\ Nm^{-1}$ was used.

2.2 Compression testing of filter samples

2.2.1 Room tempered and heated filter samples

Cylindrical samples with a diameter of ~ 50 mm were cut from commercial size filters with a thickness of 50 mm, using a diamond bit core drill with water as the cooling medium. After cutting the filter samples were dried at 100 °C overnight, with subsequent measurements of the exact dimensions and weight enabling calculations of the foam density of the sample. The compression testing was performed using an 880 Hydraulic Tensile Testing Machine (MTS, USA) with 50mm diameter pistons as seen in Figure 1 (a), at 2 mm/min compression speed. Trials were run until the first peak in applied load was registered, as that was decided to represent total failure of the foam as in earlier studies performed by other researchers [4–9]. The compression strength was calculated by using the following relationship:

$$\sigma_{fc} = \frac{F_{max}}{A} \tag{5}$$

where F_{max} represents the peak load and A the loaded area.

The effect of temperature and holding time was initially investigated, with testing at room temperature and later at operating temperature with varying duration of sample preheating, see .

Table 1. The number of tests performed per holding time at operating temperature is also included in the table.

Table 1: Experimental variations for the compression tests performed at both room- and operating temperatures for aluminium filtration.

Testing condition	Room temperature	Operating temperature		
Temperature at the start of the test	25 °C	730 °C	730 °C	730 °C
Duration of heating	-	10 minutes	1 hour	2 hours
Number of samples tested	22	10	10	10

For the compression testing at operating temperature the filter samples were heated in a resistance furnace at 800 °C prior to testing, see Figure 1 (b). The temperature development within the filter samples was measured by the use of a K-type thermocouple in 4 different filter samples, see Figure 1 (c). It was established that the samples reached a temperature of 800 °C after ~ 8 minutes in the furnace, meaning that the samples with the shortest holding time (10 minutes) would have just reached 800 °C upon retrieval. Furthermore, the temperature decreased quite rapidly in air after retrieval from the furnace, which resulted in a sample temperature of ~ 730 °C at compression.

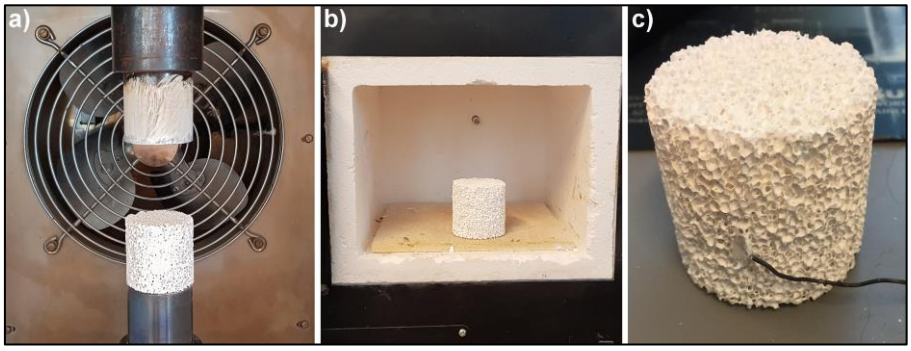

Figure 1: Images from the experimental procedure at room temperature, as well as at operating temperature where (a)) shows the compression test apparatus with a filter sample between the pistons, (b) a filter sample in the furnace used to heat the samples to 800°C, and (c) how the thermocopuple was pierced into a filter sample to measure the temperature development.

2.2.2 Filter samples submerged in molten aluminium

Achieving submersion of CFFs in aluminium, which includes complete soaking of the filter to simulate the flow of aluminium through the filter, is a complicated process that requires an outer force pushing the molten metal into the pores of the filter an thereby priming the filter.

In the present study an electromagnetic field of ~ 0.2 T (measured in the centre of an empty coil with a Hall Effect gauss meter, model 6010 by Pacific Scientific OECO, F.W. Bell®, USA), generated by a double layered water-cooled copper coil, was used to submerge the samples in aluminium and thereby securing that the molten metal had entered into every pore of the filter sample. The coil, positioned around the molten metal bath and the filter sample, was connected to a step-down power transformer (230/30-26-21-17-15 V at 45 kVAr) delivering a nominal voltage of 28 V and a current of 747A at the used power ratio (230/30 V). The experimental priming set-up is based on patented technology developed at the lab of the Department of Materials Science and Engineering, Norwegian University of Science and Technology (NTNU) [2,17,18].

The preheated filter samples were submerged separately in ~ 550 grams of pure molten aluminium (99.8 wt-% Al) at ~750 °C. Although full submersion was achieved almost instantly, the electromagnetic field was applied for 5 minutes for all samples. Melt solidification, with the filter samples fully submerged in the aluminium as seen in Figure 2 (a),

occurred seconds after the electromagnetic field was turned off. A longer priming duration would have required extra measures such as insulation to avoid premature solidification, due to the low amount of molten metal.

The main difference between the compression tests performed at room temperature and those performed on preheated filters, was the use of a sample holder allowing the testing of the submerged filters as can be seen in Figure 2 (b) and (c). The sample holder was made from a welded steel container specifically designed for the purpose, with a groove to fit on top of the bottom piston in the MTS 880 unit and a container to hold the aluminium melt. Additionally, the inside of the holder was filled with MASTIC 85 refractory ceramic fibres (Pyrotek® Inc., USA) to perfectly fit the shape of the primed metal sample, and then coated with boron nitride (BN) on the surface. The metal sample and the sample holder were put into the resistance furnace at 750 °C and left there until the metal was melted and the desired temperature reached, see Figure 2 (b). The aluminium melt was then skimmed just before initiating the compression test. The compression rate was 2 mm/min, which was the condition used for all the tests regardless of test temperature, until melt solidification (represented by a sample post compression in Figure 2 (d)). Additionally, a reference test with only pure aluminium was performed using the same procedure as described above, skipping the filter priming step and instead melting only aluminium in the sample holder directly.

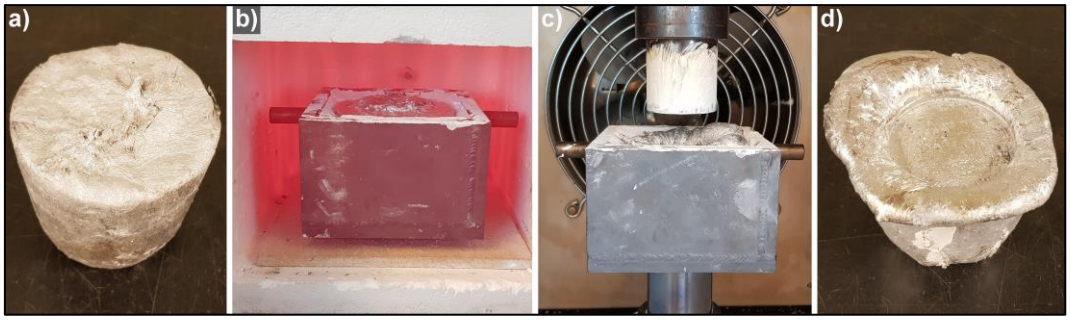

Figure 2: Images from the experimental procedure of filter samples submerged in molten aluminium where (a)) shows the solidifed metal with a primed filter within before testing, (b) the sample holder containing the filter sample and molten aluminium in the furnace, (c) how the sample holder was set between the pistons, and (d) the solidified metal with a filter within after compression.

3. Results and Discussion

3.1 As-received filter characterisation

The chemical analysis of the filter using energy-dispersive X-ray microanalysis (the limited accuracy of this method should be noted), indicated that it is alumina-based (Al_2O_3) as expected with low amounts of phosphorus (P) and silicon (Si). Observations using scanning electron microscopy revealed a relative dense microstructure consisting of tiny pores evenly distributed within the struts. Additionally, large triangular holes in the strut centres where the polyurethane skeleton had been before being burned off was observed, presented by the white arrows in Figure 3. Further observations were a few unevenly distributed larger pores observed in the struts, pointed out by the blue arrows in Figure 3, as well as a variation in size of the triangular holes. All the observed porosity can directly be correlated to what was described as pre-existing flaws in the literature, while the variation in size of the triangular holes can also be an effect of where the filters were cut before analysis.

The densities of the cut and tested filter samples are presented in Table 2. The foam density is based on the measured macro-dimensions and the weight of each sample, while the material density was measured on representative pieces of the filter samples with the use of a mercury intrusion porosimetry unit. The measured values for the material density was

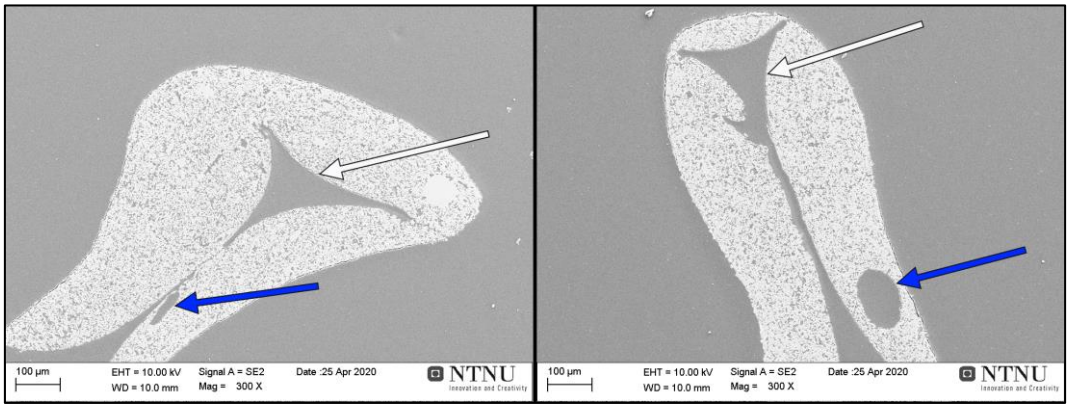

Figure 3: Scanning electron microscopy images showing the microstructure and apparent porosity of struts in as-received CFFs. The white arrows highlight the hollow strut centres triangular in shape, while the blue arrows highlight large pores that seem randomly distributed.

assumed to represent the bulk density of the solid in which the filters were made of. The relative density was calculated by dividing the average foam density with the average material density, and the strut thickness was based on measurements obtained by using a digital microscope. The standard deviations for the different values presented in Table 2 shows that there are some variation in the foam density between the filter samples, but within acceptable limits as the standard deviation is 6.4 % of the average value. The standard deviation for the strut thickness is, on the other hand, very large and can be described by a variation in strut size. Furthermore, the average relative density of the filter samples is relatively low given that it for a solid sample would have been 1.

Table 2: Different density properties of the cut filter samples. All values are given as an average, as well as with standard deviations were applicable.

Foam density (ρ_{foam}) [g/cm^3]	**Material density (ρ_{solid}) [g/cm^3]**	**Relative density (ρ_{foam} / ρ_{solid})**	**Strut thickness [µm]**
0.40 ± 0.03	2.15 ± 0.02	0.19	291 ± 73

3.2 Compression testing of filter samples

Representative load-displacement curves measured during the compression testing of the filter samples (i) at room temperature, (ii) heated with a holding time of 10 minutes, (iii) submerged in molten aluminium, as well as for (iv) a reference with aluminium only, are presented in Figure 4. As can be seen from the figure, the curves at room temperature and operating temperature partly bear a resemblance to the two first regions linear elasticity and collapse as proposed by Ashby [3]. There is a sharp linear increase initially that correlates well to the bending of the struts, but there are also several drops in the applied load indicating single struts breaking without an overall failure of the foam, as other researchers have reported earlier [6–9], and thus the region is not elastic. The slope of the linear region of both curves is about 7 kN/mm at an $R^2 > 0.9$, indicating similar behaviour between the two conditions. Foam overall failure and collapse, without a plateau as proposed by Ashby [3], clearly occurs at the curve peak as there is a major drop in the applied load of approximately 95 % under both conditions. Thus, the maximum value of the load measured represents the foam's compression strength. It can also be seen from Figure 4 that a difference in the peak load exists between the samples at room temperature and those at operating temperature, which can be explained by natural variations as only one curve of each is presented. As the slope and shape of both curves are similar, there are no indications that heating filters for 10minutes has any impact on their compressive behaviour.

The curve seen in Figure 4 that represents the filter sample submerged in aluminium is similar in shape to the previous curves, but with an experimental scatter that is both more pronounced and more frequent. The latter could be explained by an increased disturbance at the load cell and thereby increased resistance due to the medium being different than air. The initial linear region of the filter sample submerged in aluminium, is however less steep with a slope of ~ 1.5 kN/mm

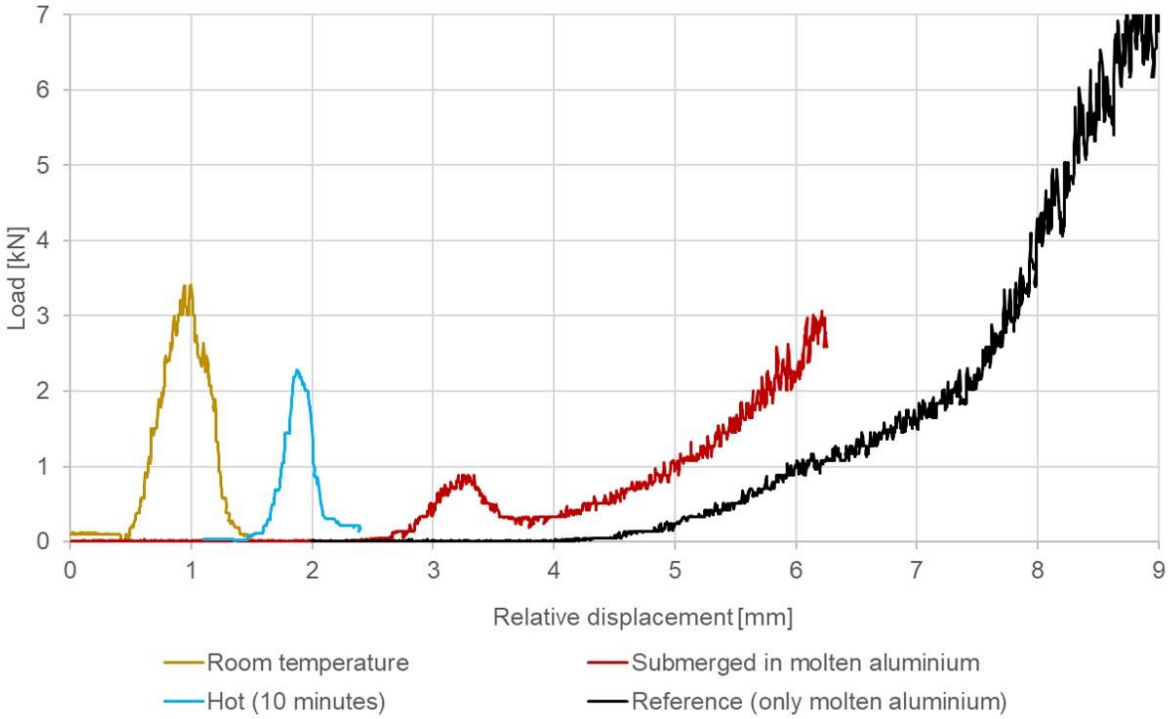

Figure 4: Representative load-displacement curves for the compression testing of a filter sample (i) at room temperature, (ii) heated with a holding time of 10 minuttes, (iii) submerged in aluminium, and for (iv) a reference with aluminium only (no filter sample). Note the relative displacement on the x-axis, meaning different starting points for different curves, but identical scale. For the two trials in aluminium there were several mm of displacement prior to an increase in load values.

at an $R^2 > 0.9$. When comparing the curves obtained for the filter samples at room temperature and at operating temperature, with slopes of ~ 7 kN/mm, the filter submerged in aluminium exhibit a far less brittle behaviour. Thus, it appears that submerging the filters in aluminium leads to a softening of the ceramic structure.

The peak seen in Figure 4 on the curve representing the filter sample submerged in aluminium is evident with a subsequent load drop of approximately 80 %. This can be correlated to overall foam failure also when compared with results previously reported in literature [6], which set the failure criterion to a force loss from the peak value at 70 %. The reduction in load drop compared to room temperature can be explained by the molten aluminium starting to solidify, visible by comparing the curve for a filter submerged in aluminium with the reference curve compressing molten aluminium only. As can be seen for the former, there is a sharp increase in the load after foam failure, and the slope of the curve further increases with the relative displacement. The curve of the reference trial with only molten aluminium (no filter sample) can be seen to have a similar shape from the moment of which the solidification starts (after ~ 80seconds, *i.e.* 2.6 mm, of displacement at 0 MPa). It can also be seen that there is a change in the slope of the curve where it is linear, which is consistent with the onset of dendrite coherency, followed by a more steep rise where the solidifying aluminium starts to develop a dendritic network that further resists compression [19].

Average compression strength together with the standard deviations for all the tested filter samples (i) at room temperature, (ii) at operating temperature with different holding times, and (iii) submerged in molten aluminium, is presented in Figure 5. As can be seen from the figure, there are differences between the filter samples tested at room temperature and those tested at 730°C, but the differences are within the standard deviation. However, a more detailed analysis of the variance based on a null hypothesis that there is no difference between the room temperature values and the operating temperature values, gave a P-value of 0.04. Thus, the null hypothesis had to be rejected, which indicates that there is a detrimental effect of the operating temperature at holding times of 1 and 2 hours, but not for a holding time of 10 minutes. This is partly in accordance with a previous study by Goretta *et al.* [11] who performed testing on a similar material at room temperature and at 800 ℃. The study found no difference in compression strength between room temperature and 30 minutes at 800 ℃ and described a decrease in compression strength above 1200 ℃ due to glass

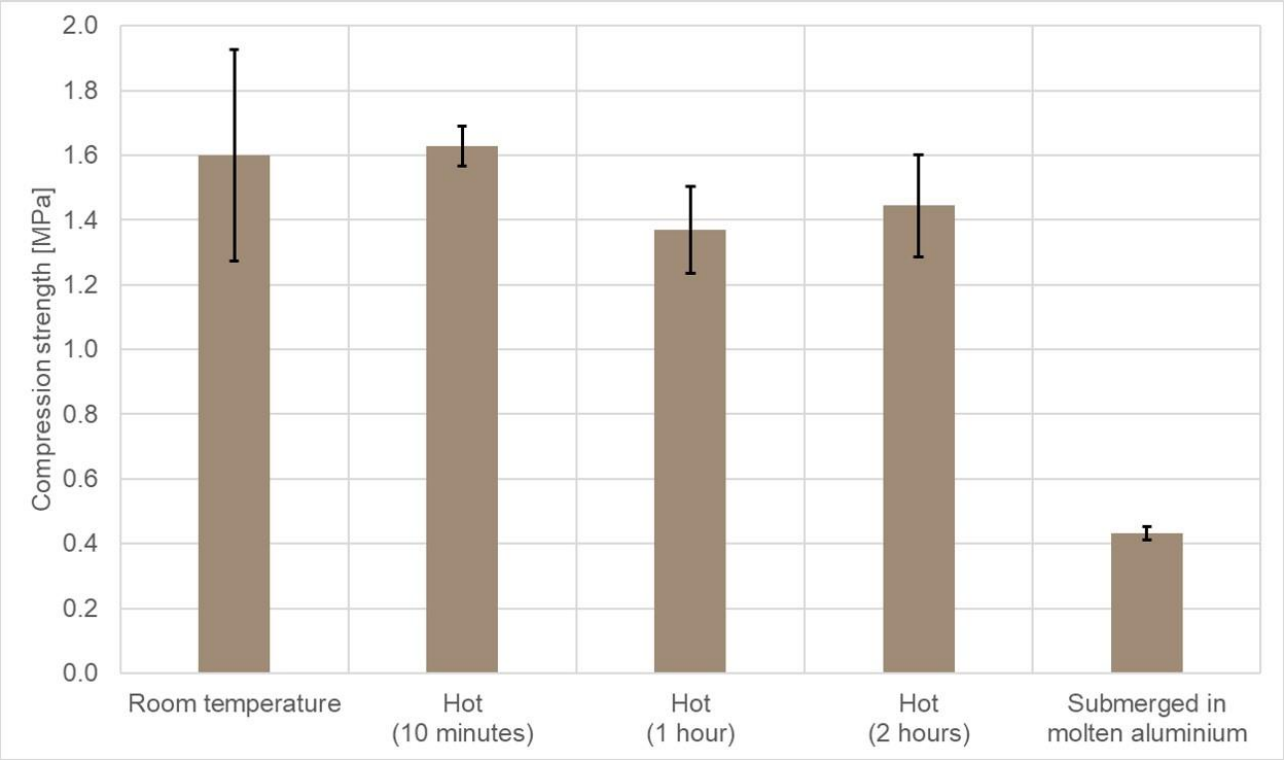

Figure 5: Average compression strength with accompanying standard deviations from testing of filter samples (i) at room temperature, (ii) at operating temperature (i.e. holding temperature of 800 °C and testing temperature of 730 °C) after heating at different holding times (10 minutes, 1 hour and 2 hours), and (iii) submerged in molten aluminium.

softening. It could, however, be that a longer holding time at 800 °C, *i.e.* 1 and 2 hours instead of 30 minutes, served the same purpose as increasing the temperature further. For the filter samples submerged in molten aluminium there was a major decrease in the compression strength from in the range of 1.37 - 1.63 MPa to 0.43 MPa, representing a decrease of ~ 68 – 73 %. Thus, the contact with aluminium has an additional detrimental effect at higher temperature which can be explained by the corrosive nature of aluminium as it leads to a reaction that weakens the ceramic structure [20]. Another possible explanation is the experimental procedure itself, where the aluminium that the filters were submerged in had to be solidified after priming before being remelted prior to compression testing. Solidification shrinkage might have introduced cracks that could have led to a reduction in the filter's tolerance for compression. This is, however, not the only explanation as the observed decrease in strength was substantial. The decrease can also not be explained by the existing variation in density, as the difference in average relative density between the tests at room temperature and those performed submerged in molten aluminium at operating temperatures was only 1 %.

It should be noted that there is a clear variation in the standard deviations observable in Figure 5, where testing of filter samples at room temperature had a significant standard deviation while testing of filter samples submerged in molten aluminium had a lower standard deviation. A possible explanation is even in this case the softening of the Al_2O_3 glassy phase, as described to occur at higher temperatures by Goretta *et al.* [11], which at 800 °C might have somewhat reduced the number of flaws in the microstructure of the ceramic foam, thus also reducing the standard deviation. In other words, with the presented average compression strengths and standard deviations in Figure 5, there are clear indications that the developed experimental procedure for testing of CFFs at operating temperature and submerged in molten aluminium show good reproducibility with realistic values.

Conclusions

In an attempt to predict the compression strength of CFFs when exposed to actual casthouse conditions, efforts were made to develop an experimental procedure for compression testing of ceramic foams at operating temperature and submerged in molten aluminium.

The resulting load-displacement curves, compression strengths and standard deviations from the developed procedures, show reasonable and realistic values with good reproducibility in comparison with testing at room temperature and with previously reported studies.

A significant decrease in compression strength was observed for CFF samples submerged in aluminium, likely due to a reaction occurring between aluminium and the CFFs, weakening their structure. A less brittle behaviour and thus a softening of the ceramic structure was also observed for the exposed filter samples compared to the unexposed samples.

Despite the fact that the results reported in the present study are preliminary (more extensive testing is presently being performed), it is believed that filter suppliers should question the relevance of the strength values measured on room tempered filters and therefore develop procedures to measure the actual strength of their filters at operating temperatures while being submerged in molten metal.

Acknowledgements

The authors would like to thank the Research Council of Norway (NFR project nr: 284090) and the German Research Foundation (DFG) for supporting these investigations as part of the Collaborative Research Centre 920 “Multi-Functional Filters for Metal Melt Filtration – A Contribution towards Zero Defect Materials” (Project-ID 169148856) subprojects A02. Furthermore, the authors would also like to acknowledge the support of Norsk Hydro ASA and the Department of Materials Science and Engineering at the Norwegian University of Science and Technology. Special thanks are given to Dr. Claudia Voigt for valuable discussions, and Kristoffer Smedal Olsen and Sara Linnea Larsson Grayston for working on this topic in their bachelor’s thesis. Appreciation is also sent to Pyrotek Sivex for supplying the CFFs.

References

[1] K. Schwartzwalder, H. Somers, A. V. Somers, Method of Making Porous Ceramic Articles, US 3,090,094, 1963.

[2] R. Fritzsch, M.W. Kennedy, J.A. Bakken, R.E. Aune, Electromagnetic Priming of Ceramic Foam Filters (CFF) for Liquid Aluminum Filtration, Light Met. (2013) 973–979. https://doi.org/10.1002/0781118663189.ch165.

[3] M.F. Ashby, Mechanical Properties of Cellular Solids., Metall. Trans. A, Phys. Metall. Mater. Sci. 14 A (1983) 1755–1769. https://doi.org/10.1007/BF02645546.

[4] S. Meille, M. Lombardi, J. Chevalier, L. Montanaro, Mechanical Properties of Porous Ceramics in Compression: On the Transition Between Elastic, Brittle, and Cellular Behavior, J. Eur. Ceram. Soc. 32 (2012) 3959–3967. https://doi.org/10.1016/j.jeurceramsoc.2012.05.006.

[5] C.Q. Dam, R. Brezny, D.J. Green, Compressive Behavior and Deformation-Mode Map of an Open Cell Alumina, J. Mater. Res. 5 (1990) 163–171. https://doi.org/10.1557/JMR.1990.0163.

[6] C. Voigt, J. Storm, M. Abendroth, C.G. Aneziris, M. Kuna, J. Hubálková, The Influence of the Measurement Parameters on the Crushing Strength of Reticulated Ceramic Foams, J. Mater. Res. 28 (2013) 2288–2299.

[7] F.A.C. Oliveira, S. Dias, M.F. Vaz, J.C. Fernandes, Behaviour of Open-Cell Cordierite Foams under Compression, J. Eur. Ceram. Soc. 26 (2006) 179–186. https://doi.org/10.1016/j.jeurceramsoc.2004.10.008.

[8] R. Brezny, D.J. Green, Uniaxial Strength Behavior of Brittle Cellular Materials, J. Am. Ceram. Soc. 76 (1993) 2185–2192. https://doi.org/10.1111/j.1151-2916.1993.tb07753.x.

[9] J. Hubálková, C. Voigt, A. Schmidt, K. Moritz, C.G. Aneziris, Comparative Phenomenological Study of Fracture Behavior of Ceramic and Glass Foams under Compressive Stress Using In Situ X-Ray Microtomography, Adv. Eng. Mater. 19 (2017) 1–9. https://doi.org/10.1002/adem.201700286.

[10] L.J. Gibson, M.F. Ashby, Cellular Solids: Structure and Properties, 2nd ed., Cambridge University Press, Cambridge, UK, 1997.

[11] K.C. Goretta, R. Brezny, C.Q. Dam, D.J. Green, A.R. De Arellano-Lopéz, A. Dominguez-Rodriguez, High Temperature Mechanical Behavior of Porous Open-Cell Al2O3, Mater. Sci. Eng. A. 124 (1990) 151–158. https://doi.org/10.1016/0921-5093(90)90145-S.

[12] W. Acchar, F.B.M. Souza, E.G. Ramalho, W.L. Torquato, Mechanical Characterization of Cellular Ceramics, Mater. Sci. Eng. A. 513–514 (2009) 340–343. https://doi.org/10.1016/j.msea.2009.02.012.

[13] R. Brezny, D.J. Green, Fracture Behavior of Open-Cell Ceramics, J. Am. Ceram. Soc. 72 (1989) 1145–1152.

[14] R. Brezny, D.J. Green, C.Q. Dam, Evaluation of Strut Strength in Open-Cell Ceramics, J. Am. Ceram. Soc. 72 (1989) 885–889. https://doi.org/10.1111/j.1151-2916.1989.tb06239.x.

[15] R. Brezny, D.J. Green, The Effect of Cell Size on the Mechanical Behavior of Cellular Materials, Acta Metall. Mater. 38 (1990) 2517–2526. https://doi.org/10.1016/0956-7151(90)90263-G.

[16] G. Heness, N. Booth, B. Ben-Nissan, Does Size Matter? - The Effect of Volume on the Compressive Strength of Open Cell Brittle Ceramics, Adv. Mater. Res. 41–42 (2008) 221–226. https://doi.org/10.4028/www.scientific.net/amr.41-42.221.

[17] M.W. Kennedy, S. Akhtar, J.A. Bakken, R.E. Aune, Electromagnetically Modified Filtration of Aluminum Melts Part I: Electromagnetic Theory and 30 PPI Ceramic Foam Filter Experimental Results, Metall. Mater. Trans. B. (2013) 1–15. https://doi.org/10.1007/s11663-013-9798-8.

[18] M.W. Kennedy, S. Akhtar, R. Fritzsch, J.A. Bakken, R.E. Aune, Apparatus and Method for Priming a Molten Metal Filter, US9605332B2, 2013.

[19] G. Chai, L. Baeckerud, L. Arnberg, Study of Dendrite Coherency in Al-Si Alloys During Equiaxed Dendritic Solidification, Zeitschrift Fuer Met. 86 (1995) 54–59.

[20] A. Bergin, C. Voigt, R. Fritzsch, S. Akhtar, L. Arnberg, C.G. Aneziris, R.E. Aune, Experimental Study on the Chemical Stability of Phosphate Bonded Al2O3-based Ceramic Foam Filters (CFFs), Submitt. to Metall. Mater. Trans. B. October (2020).